



Calculation of optimum feed-line impedance of series-fed microstrip antennas using the image parameter method and Bloch theory

Ji-Yeon Ha¹ · Dong-Wook Seo[†]

(Received December 21, 2022 : Revised January 19, 2023 : Accepted March 19, 2023)

Abstract: In millimeter-wave bands, microstrip array antennas are used for various communications and sensors because of their lightweight and low cost. A series-fed method that can reduce the length of a feed line as much as feasible is preferable over a parallel feed method to reduce the loss in a microstrip array antenna. However, the characteristic impedance, which is simple to fabricate without a theoretical analysis or comprehension, is primarily chosen and applied to the feed line of the microstrip array antenna. In this paper, we propose an optimal feedline selection method for a series-fed microstrip array antenna using the image parameter method and Bloch theory, both of which are used in filter design in microwave engineering. A typical 79 GHz band series-fed microstrip array antenna has a gain of 14.7 dB with a preferred feed line of 100 Ω , whereas a gain of 17.3 dB with the characteristic impedance calculated using the image parameter method and Bloch theory. The proposed method resulted in a 1.3 dB increase in antenna gain. These results are preliminary from the simulations, and prototypes will be fabricated in the future to verify the proposed method.

Keywords: Array antenna, Feed line, Microstrip antenna, mmWave

1. Introduction

In the past, the millimeter-wave (mmWave) band was primarily used for military radar systems; however, it has recently been developed and expanded for civilian use, such as vehicle radars [1]. Furthermore, as 5G communication began service in the mmWave band, market attention has focused on the mmWave band [2].

Various types of antennas have been used in the mmWave bands, such as microstrip patch antennas, slotted waveguide antennas, and antennas with lenses or reflectors. Reflector antennas generally have a very low loss, but they have a large volume and limited bandwidth because they require separate layers for reflection and an excitation antenna for the incident. Slotted array waveguide antennas are highly efficient, can easily distribute open-surface power, and are structurally robust. However, combining antennas with other radiofrequency (RF) modules is difficult, and the antenna size becomes extremely small at high frequencies in the sub-THz band, making manufacturing difficult [3]. However, microstrip patch antennas are lightweight owing to their thin substrates [4]-[7].

Nevertheless, certain drawbacks exist, including a low power-handling capability, low gain, and narrow bandwidth. In particular, conductor and dielectric losses rapidly increase at high frequencies above the microwave band, limiting its use. However, as hardware performance and signal processing algorithms improve, antenna gain requirements are reduced. Consequently, this has regained the popularity of microstrip array antennas in the mmWave band [8].

The majority of losses in microstrip antennas are caused by dielectric and conductor losses that are proportional to the total printing pattern length. Therefore, the shorter the length of the entire feed line, the smaller the loss. The series feeding method is preferred over the parallel feeding method in mmWave microstrip array antennas that are vulnerable to loss [9][10].

In the series feeding method for microstrip array antennas, the characteristic impedance is often used as an approximate value rather than an accurately calculated value. A feed line of 100 Ω , the feed line width for fabrication convenience, is commonly used in series-fed microstrip array antennas operating at 77 GHz or 79 GHz [11]-[13]. That is, theoretical research or analysis on

[†] Corresponding Author (ORCID: <http://orcid.org/0000-0001-9449-7772>): Professor, Division of Electronics and Electrical Information Engineering / Interdisciplinary Major of Maritime AI Convergence, Korea Maritime & Ocean University, 727, Taejong-ro, Yeongdo-gu, Busan 49112, Korea, E-mail: dwseo@kmou.ac.kr, Tel: +82-51-410-4427

1 M. S. Candidate, Interdisciplinary Major of Maritime AI Convergence, Korea Maritime & Ocean University, E-mail: su000721@g.kmou.ac.kr, Tel: +82-51-410-4427

This is an Open Access article distributed under the terms of the Creative Commons Attribution Non-Commercial License (<http://creativecommons.org/licenses/by-nc/3.0>), which permits unrestricted non-commercial use, distribution, and reproduction in any medium, provided the original work is properly cited.

the feed line width of the series feeding method is lacking.

A microwave filter is a two-port network with a periodic structure that has a frequency response at a specific point in the RF owing to attenuation in the stopband, providing transmission at frequencies within the passband [14]. The image parameter method and Bloch theory are used to design the input and output impedances of a filter with a periodic structure. In this study, using the image parameter method and Bloch theory, we attempt to determine the optimal feed line for a series-fed microstrip array antenna with several radiating elements arranged in a periodic structure.

2. Proposed methods

2.1 Image parameter method

Consider a two-port network characterized by its ABCD parameters, as shown in **Figure 1**. Image impedance Z_{i1} is the input impedance at port 1 when port 2 is terminated with Z_{i2} , and image impedance Z_{i2} is the input impedance at port 2 when port 1 is terminated with Z_{i1} .

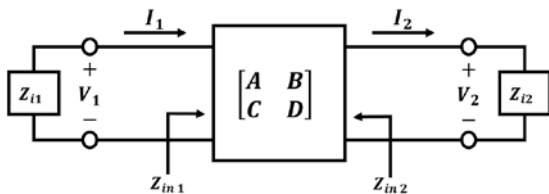


Figure 1: Two-port network terminated in its image impedance

In a two-port network, the two ports are matched when terminated with their image impedance. In terms of the ABCD parameters of the network, the image impedances of ports 1 and 2 are expressed in [14] as follows:

$$Z_{i1} = \sqrt{AB / CD} , \quad (1)$$

$$Z_{i2} = \sqrt{BD / AC} . \quad (2)$$

If the network is symmetric, $A = D$ and $Z_{i1} = Z_{i2}$.

2.2 Bloch theory

Consider a periodic loading line of infinite length, as shown in **Figure 2**. Depending on the frequency and normalized susceptance values, the periodic line represents passbands or stopbands and thus can be considered as a type of filter. Each unit

cell of this line consists of a transmission line of length d with shunt susceptance b that is normalized to characteristic impedance Z_0 ; k is the propagation constant. Here, I_n and I_{n+1} represent the currents on both sides of the n th and $n+1$ th unit cells, respectively. Similarly, V_n and V_{n+1} represent the voltages on both sides of the n th and $n+1$ th unit cells, respectively.

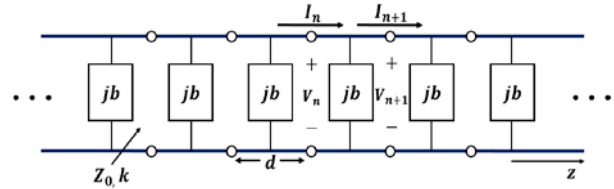


Figure 2: Periodically loaded transmission line's equivalent circuit

If the finite line comprises a cascade connection of identical two-port networks, we determine the relationship between the voltages and currents on both sides of the n th unit cell using the ABCD matrix as follows:

$$\begin{bmatrix} V_n \\ I_n \end{bmatrix} = \begin{bmatrix} A & B \\ C & D \end{bmatrix} \begin{bmatrix} V_{n+1} \\ I_{n+1} \end{bmatrix} . \quad (3)$$

The characteristic impedance at the end of the unit cell is called the Bloch impedance that is expressed in [14] as follows:

$$Z_B^\pm = \frac{-2BZ_0}{A - D \mp \sqrt{(A + D)^2 - 4}} . \quad (4)$$

For symmetric unit cells, $A = D$; thus, **Equation (4)** can be simply expressed as follows:

$$Z_B^\pm = \frac{\pm BZ_0}{\sqrt{A^2 - 1}} , \quad (5)$$

where \pm solutions imply the characteristic impedance of traveling waves in positive and negative directions. Except for the sign, these impedances are the same for symmetric networks. However, (5) can be used for periodic structures; but the structure need not have infinite unit cells.

3. Simulation results

To apply the proposed methods, HFSS, a commercial finite element method simulation tool for electromagnetic structure

analysis, was used to analyze the radiating elements and design the antenna. Isola Astra MT77 was used as a substrate, and it had a relative permittivity (ϵ_r) of 3.0, loss tangent ($\tan \delta$) of 0.0017, and thickness (h) of 0.127 mm.

3.1 Calculating feed-line impedance through unit cell analysis

Among the various radiating element shapes, the simplest rectangular patch was selected as the radiating element in this study. Because the electromagnetic field is concentrated between the signal pad and the ground pad, a lumped port, which is more suitable than a wave port, was used for the analysis. As shown in **Figure 3**, two lumped ports were attached to both sides of the radiating element, and the design parameters of the radiating element were optimized to resonate at an operating frequency of 79 GHz and maximize the antenna gain of a single radiating element. The optimized design parameters a , b , A , and B were 1.06 mm, 0.79 mm, 2.37 mm, and 3.18 mm, respectively.

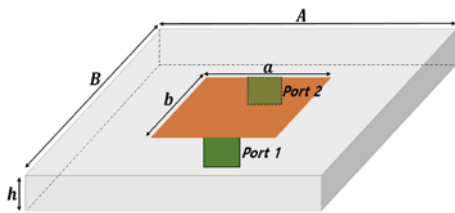


Figure 3: Simulation setup for S parameters of a rectangular radiating element

To obtain the ABCD parameters, we assumed the radiating element to be a unit cell and converted the S parameters of the optimized radiating element, as shown in **Figure 4**, to the ABCD parameters.

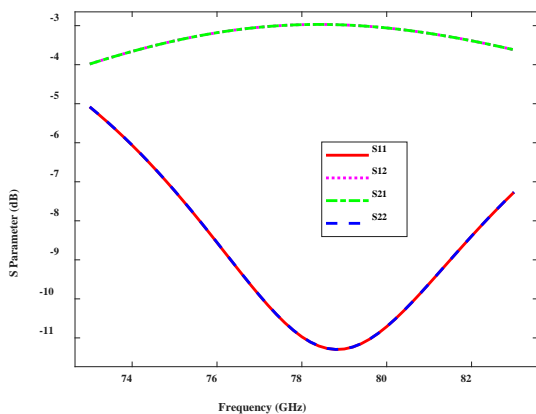


Figure 4: Simulated reflection coefficient of the unit cell

By substituting the complex values of the ABCD parameters in **Table 1** into **Equations (1)** and **(4)**, we obtained the image and Bloch impedances. The result of the image impedance was the same as that of the Bloch impedance, and the absolute and real values of the calculated optimum impedance were 119Ω and 90Ω , respectively.

Table 1: ABCD parameters of the unit cell at 79 GHz

A	B	C	D
$-0.95 - 0.24j$	$8.05 - 82.6j$	$-0.01 - 0.00j$	$-0.94 - 0.24j$

3.2 Performance of a series-fed microstrip array antenna depending on the feed line

A conventional microstrip array antenna is required to verify the effect of the feed line on the performance of a series-fed microstrip. As shown in **Figure 5**, the rectangular radiating elements were arranged on the dielectric substrate at half-wavelength intervals ($\lambda_g/2$) and directly connected to the feed line. Therefore, all the radiating elements had the same phase characteristics. The end radiating element was connected to the inset-type feed line to match the feed line to the input impedance of the radiating element. Therefore, the inset-related parameters, w_i and $depth$, depended on the feed line. The series-fed microstrip array antenna consists of 16 identical rectangular radiating elements and a single inset-fed radiating element.

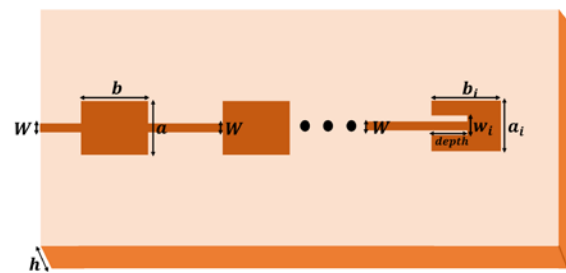


Figure 5: Geometry of a series-fed microstrip array antenna

The feed line width (W) of 119Ω , which is the absolute value of the result obtained from the image parameter method and Bloch theory, was 0.054 mm on the Astra MT77 substrate at 79 GHz. The design parameters of the corresponding end radiating element were as follows: $a_i = 0.56$ mm, $b_i = 1.071$ mm, $depth = 0.485$ mm, and $w_i = 0.137$ mm. For the feed line of 90Ω , which is the real value of the optimum impedance obtained from **Equations (1)** and **(5)**, the line width (W) was 0.11 mm, and the matched end radiating elements had the following design

parameters: $a_i = 0.562$ mm, $b_i = 1.07$ mm, $depth = 0.487$ mm, and $w_i = 0.15$ mm. When the characteristic impedance was 100Ω , which is a common width in the literature for series-fed microstrip array antennas, the width of the feed line (W) was 0.08 mm. The design parameters for a series-fed microstrip array antenna with a characteristic impedance of 100Ω were as follows: $a_i = 0.69$ mm, $b_i = 1.0595$ mm, $depth = 0.5$ mm, and $w_i = 0.16$ mm.

The simulated reflection coefficients of these series-fed microstrip array antennas are shown in **Figure 6**. The -10 dB reflection coefficient bandwidth of the simulation was 5.74 GHz at 119Ω , 4.02 GHz at 90Ω , and 5.52 GHz at 100Ω . Notably, the feed line with an optimum characteristic impedance of 119Ω increased the bandwidth by approximately 200 MHz compared with the common characteristic impedance of 100Ω . Moreover, we note that the absolute value, rather than the real value, of the impedance obtained from the Bloch theory and image impedance method should be used as the impedance of the feed line.

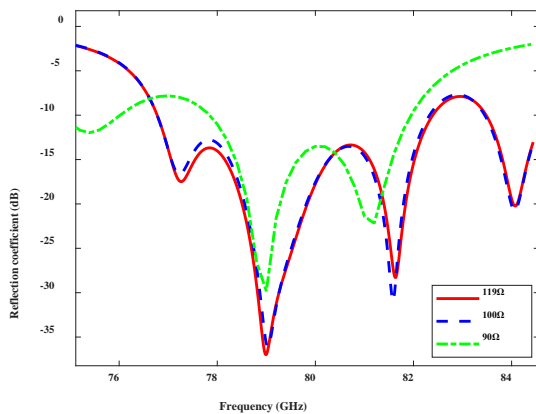
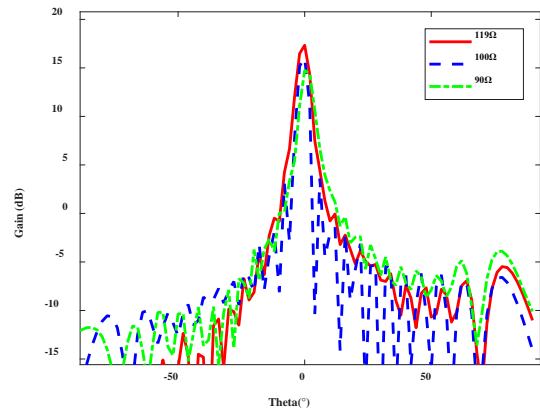


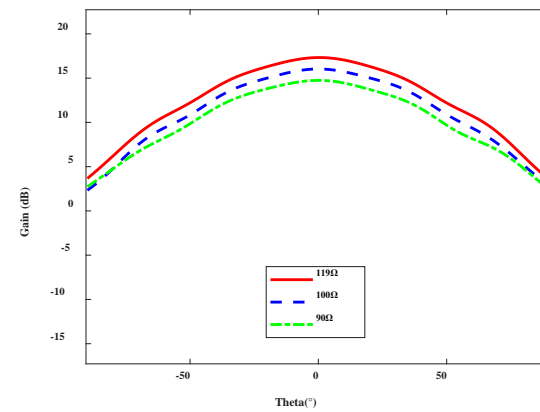
Figure 6: Simulated reflection coefficients of the antenna with respect to the operating frequencies

The radiation patterns of the E- and H-planes simulated at 79 GHz are shown in **Figure 7**. The peak gains in the E- and H-planes were 17.33 dB for the characteristic impedance of 119Ω with a feed-line width of 0.054 mm, 14.75 dB for the characteristic impedance of 90Ω with a feed-line width of 0.11 mm, and 16.02 dB for the characteristic impedance of 100Ω with a feed-line width of 0.08 mm.

The simulated antenna efficiency is shown in **Figure 8**. The antenna efficiencies were 97.55% , 96.13% , and 94.98% at 119Ω , 100Ω , and 90Ω , respectively. The highest antenna efficiency was obtained using a 119Ω feed line.



(a)



(b)

Figure 7: Simulated radiation patterns at 79 GHz: (a) E-plane; (b) H-plane

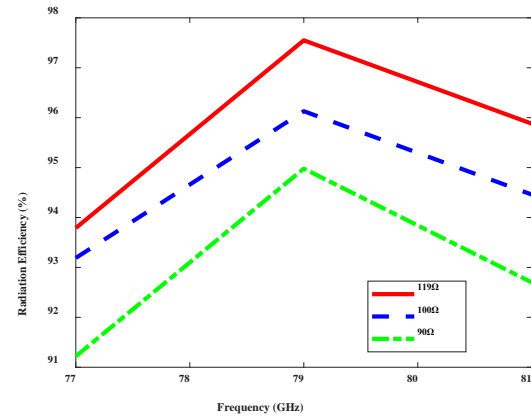


Figure 8: Simulated antenna efficiency at the operating frequency

For a feed line with a characteristic impedance of 119Ω , the antenna gain was approximately 1.31 dB higher than that of a series-fed microstrip array antenna with a feed line of 100Ω . Furthermore, the gain when using a feed line with a characteristic impedance of 119Ω was approximately 2.58 dB higher than that

when using a feed line with a characteristic impedance of 90Ω . That is, when the absolute values of the optimal characteristic impedances obtained from the image parameter method and Bloch theory are applied, a larger antenna gain can be obtained than when the real values are applied.

The difference in gain between the characteristic impedances of 119Ω and 100Ω was linearly approximately 1.35 times; this is an effect that can theoretically reduce the number of radiating elements by 1.35 times compared with the conventional method. Therefore, the feed line of 100Ω required 23 radiating elements to have the same gain as the series-fed microstrip array antenna with a feed line of 119Ω and 17 radiating elements.

4. Conclusion

In this study, we propose an optimal feedline selection method for a series-fed microstrip array antenna operating in the mmWave band. A microstrip array antenna using the proposed feed-line selection method was implemented on a dielectric substrate at a center frequency of 79 GHz, and the reflection coefficient and radiation pattern were simulated. When the gain of the proposed feed-line selection method was compared to that of the conventional feed line, the gain of the proposed method was approximately 1.31 dB higher. We hope that the proposed method provides a good criterion for determining the feed lines of series-fed microstrip array antennas. In future work, we plan to fabricate conventional and designed series-fed array antennas and verify the feasibility of the proposed method by comparing our designed antenna with the conventional antenna.

Acknowledgement

This research was supported by Basic Science Research Program through the National Research Foundation of Korea(NRF) funded by the Ministry of Education(2021R111A3044405).

Author Contributions

Conceptualization, D.-W. Seo; Methodology, J.-Y. Ha and D.-W. Seo; Software, J.-Y. Ha; Formal Analysis, J.-Y. Ha; Investigation, J.-Y. Ha; Resources, J.-Y. Ha; Data Curation J.-Y. Ha; Writing-Original Draft Preparation, J.-Y. Ha; Writing-Review & Editing, D.-W. Seo; Visualization, J.-Y. Ha; Supervision, D.-W. Seo; Project Administration, D.-W. Seo; Funding Acquisition, D.-W. Seo.

References

- [1] S. -H. Lee, J. -H. Lee, and D. -W. Seo, "mmWave band microstrip comb-line array antenna for a low sidelobe level," *The Journal of Korean Institute of Electromagnetic Engineering and Science*, vol. 31, no. 10, pp. 855-862, 2020 (in Korean).
- [2] Y. C. Chang, C. -C. Hsu, M. I. Magray, Y. -C. Hsu, and J. -H. Tarn, "Wideband and low profile miniaturized magneto-electric dipole antenna for 5g mmWave applications," *2020 IEEE Asia-Pacific Microwave Conference (APMC)*, pp. 697-699, 2020.
- [3] Y. -P. Lee, J. -M. Lee, J. -S. Bang, T. -Y. Jung, J. -S. Lee, D. -H. Lee, H. -S. Lyu, and K. -C. Hwang. "Gap-coupled series-fed millimeter-wave array antenna for automotive radar applications," *The Journal of Korean Institute of Electromagnetic Engineering and Science*, vol. 31, no. 4, pp. 394-397, 2020 (in Korean).
- [4] Z. Cao, Z. Liu, H. Meng, and W. Dou, "Design of W-band microstrip antenna array," *2019 IEEE Asia-Pacific Microwave Conference (APMC)*, pp. 1319-1321, 2019.
- [5] J. FangFang and D. -K. Park, "Design of a miniaturized monopole antenna for UWB application," *Journal of Advanced Marine Engineering and Technology*, vol. 44, no. 6, pp. 482-486, 2020.
- [6] J. -I. Lee, J. -H. Lee, S. -H. Lee, and D. -W. Seo, "Low sidelobe design of microstrip comb-line array antenna using deformed radiating elements in the millimeter-wave band," *IEEE Transactions on Antennas and Propagation*, vol. 70, no. 10, pp. 9930-9935, 2022.
- [7] J. -H. Lee, S. -H. Lee, H. J. Lee, J. -H. Oh, J. -Y. Kim, I. -K. Cho, and D. -W. Seo, "Design of comb-line array antenna for low sidelobe level in millimeter-wave band," *IEEE Access*, vol. 10, pp. 47195-47202, 2022.
- [8] S. Sugawa, K. Sakakibara, N. Kikuma, and H. Hirayama, "Low-sidelobe design of microstrip comb-line antennas using stub-integrated radiating elements in the millimeter-wave band," *IEEE Transactions on Antennas and Propagation*, vol. 60, no. 10, pp. 4699-4709, 2012.
- [9] S. Ghosh and D. Sen, "An inclusive survey on array antenna design for millimeter-wave communications", *IEEE Access*, vol. 7, pp. 83137-83161, 2019.
- [10] A. Pandey, *Practical Microstrip and Printed Antenna Design*, Norwood, MA, USA: Artech House, 2019.

- [11] J. -H. Lee, J. M. Lee, and K. C. Hwang, "Series feeding rectangular microstrip patch array antenna for 77 GHz automotive radar," 2017 International Symposium on Antennas and Propagation (ISAP), pp. 1-2, 2017.
- [12] A. Liu, W. Wang, J. Wang, M. Guo, and L. Zhao, "A single-layer series-fed microstrip array with enhanced bandwidth for automotive radar systems," 2018 IEEE International Symposium on Antennas and Propagation & USNC/URSI National Radio Science Meeting, pp. 1737-1738, 2018.
- [13] S. Karuppuswami, S. Mondal, and P. Chahal, "Design optimization of a 77 GHz antenna array using machine learning," 2021 IEEE 71st Electronic Components and Technology Conference (ECTC), pp. 1199-1204, 2021.
- [14] D. M. Pozar, Microwave Engineering, 4th edition: John Wiley & Sons, Ch. 8, pp. 388-389, 2011.